RESONANTLY COUPLED ACCELERATING STRUCTURES FOR HIGH-CURRENT PROTON LINACS*

B. C. Knapp, E. A. Knapp, G. J. Lucas, and J. M. Potter

University of California, Los Alamos Scientific Laboratory
Los Alamos, New Mexico

Summary

The results of model studies and an equivalent circuit analysis of the operation of a chain of cavities in the $\pi/2$ mode is given. Various $\pi/2$ mode structures are described and the performance of models of these structures is discussed. Results of numerical solutions to an equivalent circuit applicable to the problem are also given, which include frequency error tolerances and coupling tolerances, for typical cases of interest. Multiple drive of a long resonator chain is also discussed.

Introduction

Accelerating structures suitable for use in a high current proton linac should have a) high stability against perturbation of the fields by beam interactions or cavity deformations, b) field amplitudes and phases which are easily controllable by drive variation, c) high efficiency in transferring RF power into particle energy d) freedom from electrical breakdown problems e) loose mechanical tolerances f) low fabricational cost. Use of the resonant $\pi/2$ mode in a periodic cavity chain as the operating point for an accelerator structure has been previously suggested[1] by this group as a choice which satisfies the above requirements. A more complete discussion of the advantages and a comparison of $\pi/2$ mode structures with other possibilities is given in Paper B-5, (E. A. Knapp, "Design, Construction and Testing of RF Structures for a Proton Linear Accelerator") of this conference. This report will discuss some geometries suitable for use as accelerator structures in this mode, and an equivalent circuit treatment of the properties of the mode, including tolerance to frequency and coupling errors in individual cells of the chain.

Model Studies

Model studies on $\pi/2$ mode structures began with cavities similar to those which would be used in 0 or π mode operation, in that the coupling cells were in the beam path. The first such model (Fig. 1) was a magnetically coupled structure with short coupling cells capacatively loaded by drift tubes. Coupling was achieved through four circular holes in the septum plate. Alternate septum plates were rotated 45° so that the direct coupling was suppressed. Operation of this cavity chain was successful. We found it possible to adjust the resonant frequencies of the two types of cavities

sufficiently well to obtain $\pi/2$ mode operation with a continuous dispersion curve through the operating point. However, it soon became apparent that the short coupling cell was subject to very stringent dimensional tolerances to attain the required frequency tolerances. Also, beam-coupling cavity interactions could be serious in this geometry. In an effort to circumvent the cavity interaction problem a second magnetically coupled structure was fabricated (Fig. 2). The coupling cells in this model were loaded with annular rings to tune the cells to resonance in the TM_{020} mode. The drift tubes in this model extend through the whole length of the coupling cell thereby eliminating interactions between the beam and the coupling field. The dimensional tolerances required to maintain a consistent resonant frequency in the coupling cell of this structure were even more difficult to achieve in the model tested than in the model of Fig. 1. However, proper operation was achieved here also. The relevant parameters for these models are shown in Table I. The Q of both models was low, because of demountable joints; Q should be approximately 20,000 with good fabrication technique. This results in a maximum shunt impedance at this β of 28 $M\Omega/M$. The values of ZT^2/Q are 80% of those expected of single cells with similar β and geometry.

A disadvantage of the iris loaded structures described above is the reduction in shunt impedance resulting from the presence of empty coupling cells in the beam path[1]. This decrease in shunt impedance comes from a decrease in both ZT^2/Q and Q for shorter cavities. To avoid this unnecessary loss in efficiency two models have been constructed which have the coupling cavity completely removed from the beam line. The first of these utilized post loaded coupling cavities on the sides of the main cells (Fig. 3).

TABLE I

Parameters for Models
of Resonantly Coupled Structures

Structure	ZT^2/Q at 805-Mc	Q	β	g/ℓ	Beam Hole Diameter
Fig. 1	1400Ω	<20,000	0.53	0.5	1.25"
Fig. 2	1450Ω	<20,000	0.55	0.5	1.25"
Fig. 3	1700Ω	16,500	0.68	0.5	1.5 "
Fig. 4	1750Ω	15,000	0.68	0.5	1.5 "

Coupling was achieved through rectangular slots in the cavity walls at the septum plate. Side coupled structures such as this have the advantages of increased shunt impedance and elimination of beam-coupling field interactions. A long model

of this structure (45 cells) was fabricated from EPT copper tubing with heli-arc brazed joints. The model was flat within ± 5% when constructed and exhibited fair Q, 16,500, but rather narrow band width, 2%. The field distribution proved to be insensitive to main cell frequency tuning. Models with larger bandwidth and better efficiency should be possible with more precise construction. Even with the narrow bandwidth very satisfactory $\pi/2$ mode operation has been achieved. The tune up procedure described in the next section was used on this model.

In an effort to improve the band width of the side coupled structures models have been constructed with resonant loops passing between accelerating cells. One successful loop coupled structure is shown in Fig. 4. The cavity loops are made an integral part of a half-wave parallel plate transmission line, whose resonant frequency may be controlled by the position of a movable shunt. Structures of this sort fabricated from ETP copper have exhibited Q's of approximately 15,000 and band widths of 8%. A long model of this type (23 cells) was fabricated. As in the previous side coupled cavity the field distribution was unaffected by changing main cell frequencies. The tank was flattened by installing tuner slugs which capicatively loaded the coupling straps near the main cell-coupling cell junction, changing the cell to cell coupling. The tank was flattened to ± 0.5% by tuning. Tuning procedure is based on the perturbation theory which was derived from the equivalent circuit analysis and is discussed later. The principal disadvantage of this structure is the low Q of the coupling system, which effectively lowers the Q of the resonant tank if frequency errors are present in the accelerating cells. This will be discussed further in the equivalent circuit section. Mechanically, this structure is complex and would prove difficult to build.

Models of resonantly coupled cloverleaf structures have been tested. The principal disadvantage of this type of cavity is the length of the coupling slot required for resonance. At 805 Mc a structure of considerably larger diameter than that which is required to meet other resonance requirements is necessary in order to accomodate these slots. The cloverleaf is desirable because of its large bandwidth (30%). Currently under test are a number of cloverleaf models with "dumbell" shaped slots. These slots are capacitively loaded in the center. These slots are shorter than the unloaded slots for a particular resonant frequency and thus require a smaller structure. However, gap tolerances and slot tuning may present problems.

The flatness and the Q of both side coupled structures have been encouraging considering the quality of the models which we have tested. Currently, we are building high-power, precision models of both side coupled structures. These models are being machined from forgings in OFHC copper.

Equivalent Circuit Analysis

Our analysis of the $\pi/2$ mode operation of periodic cavity chains is based on the analogy between a chain of coupled resonators and a chain of magnetically coupled resonant circuits (1,2, 3,4). The mesh equations for the chain of coupled circuits shown in Fig. 5 are

$$E_n = (R_n + \frac{1}{j\omega C_n} + j\ \omega 2L_n)\ i_n + j\omega M_n i_{n+1} + j\omega M_{n-1} i_{n-1} \quad (1)$$

which may be rewritten in terms of more general properties of the resonators;

$$\frac{Y_n}{2_j \omega} = (1 - (\frac{\omega_n}{\omega})^2 - j\ \frac{\omega_n}{\omega Q})X_n + \frac{K_n}{2} X_{n+1} + K_{n-1}/2 X_{n-1} \quad (2)$$

where $Y_n = \frac{E_n}{\sqrt{L_n}}$ $X_n = i_n \sqrt{L_n}$ $K_n = M_n / \sqrt{L_n L_{n+1}}$

The X_n's are the square roots of the stored energy and may be identified with the field levels in the cavities, Y_n is characteristic of the drive in the nth cell, and the K_n's are coupling strengths between cavities.

Solving for X_{n+1} in the case of no drive

$$X_{n+1} = \frac{-2}{W(n)K_n} (1 - (\frac{\omega_n}{\omega})^2 - j/Q_n(\frac{\omega_n}{\omega}))X_n - \frac{K_{n-1}}{K_n} X_{n-1} \quad (3)$$

where $W(n) = (1 + \delta_n^1 + \delta_n^N)$ and $K_0 X_0 = 0$.

From this set of equations we have deduced a procedure which has proven quite effective in tuning $\pi/2$ mode models. Also we have been able to make semi-quantitative observations on the local effects of variations in cell frequencies, coupling constants, and Q's which agree with computed observations, experimental evidence and the more complete perturbation analysis.[2]

From (3) it is clear that when X_n is real and X_{n-1} is imaginary (i.e. $\pi/2$ mode), X_{n+1} will be at a minimum and imaginary when $\omega_n = \omega$, the resonant driving frequency. Similarly, when X_n is imaginary and X_{n-1} real, X_{n+1} will be real, and 180° out of phase with X_{n-1} when $\omega_n = \omega$. Thus a $\pi/2$ mode structure driven in cell N may be tuned up by alternately adjusting the nth accelerating cell frequency for minimum field in the $(n-1)$th coupling cell and then the coupling cell for 180° phase shift between the two adjacent accelerating cells, proceeding from cell one to the driven end of the structure. Since the variations in coupling cell frequency are ordinarily not large enough to cause an appreciable cell-to-cell phase error we can conveniently converge on a "tuned-up" condition by first tuning for minimum coupling field, then for minimum phase error, and finally for minimum coupling field again. This sequence is usually sufficient to insure a tuned

up tank. Because the field in the coupling cells increases linearly toward the drive to provide power flow, the field minimum becomes increasingly obscure as one proceeds toward the drive. More accurate tuning of the last half of the tank may be achieved by reversing the position of the drive from the Nth cell to the first cell and tuning from the opposite end. The phase measurements must be rather carefully made since the errors to be corrected will rarely exceed a few degrees. The drive frequency must remain constant through this procedure. This tuning technique is described briefly in reference 1. It should be noted that the principal effect of this tune-up procedure is to maximize the Q of the structure since minimizing the field in the coupling cells (which have a lower Q) reduces the total losses. The cell-to-cell phase errors in $\pi/2$ mode structure constructed with reasonable precision should be extremely small.

For a perfectly symmetric structure it can be shown from equation (3) that if the drive is located in cell N, the ratio of coupling cell field to accelerating cell field is approximately

$$X_{2n}/X_{2n-1} \cong j(2n-1)/kQ_a$$

and that the accelerating field is constant except for a small droop away from the drive given by

$$X_{2n+1}/X_{2n-1} \cong 1+(2n-1)/K^2 Q_a Q_c$$

where Q_a is the accelerating cell Q and Q_c is the coupling cell Q. Thus the end-to-end droop can be found by summing over the tank.

$$(X_N-X_1)/X_N = (N-1)^2/4K^2 Q_a Q_c$$

For a typical structure (N=81, k=0.02, Q=20,000) driven at the end the tilt is about 2%. Since the tilt goes approximately as N^2 driving in the center of a tank reduces the tilt by a factor of four over the end driven case. Now consider equation (3) for a perfectly symmetric structure except for a small perturbation in $K_{n-1} = K + \delta K_{n-1}$. It is easily shown that

$$\delta X_{n+1}/X_{n+1} = \delta K_{n-1}/K$$

This error is propagated down the tank resulting in a field distribution similar to that shown in Fig. 6.

Numerical Studies of Chains of Coupled Resonators

The calculation of the currents in a chain of circuits (equation 2) is particularly well suited to numerical solution. The matrix for the chain has all zero terms except for the terms $a_{n,n}$, $a_{n,n+1}$, $a_{n+1,n}$. The solution of such a tridiagonal matrix is straight-forward if one solves the entire chain in terms of the first term a_{11}.

$$X_n = A_n \cdot X_1 + B_n$$

Solving the nth equation for X_{n+1} results in a series of equations which generate the A_n's and B_n's if we assume $X_1=1$.

$$X_{n+1} = \frac{-2}{K_n} \left\{ (1 - \frac{\omega_n^2}{\omega^2} - j\frac{\omega_n}{\omega}\frac{1}{Q_n})X_n + \frac{K_{n-1}}{2}(X_{n-1}) - \frac{Y_n}{2j\omega} \right\}$$

The last two equations from the matrix are both soluble for X_n, the field in the last cell. Eliminating X_n gives a unique solution for X_1, which will normalize X_n to the proper value. The accuracy of this method may be demonstrated by the symmetry of the results obtained on a digital computer for tuned up cases. The amplitudes of symmetrically located cells are identical to 10 significant figures and the phases are identically equal to the analytically obtained values even for a case with 7469 cells.

In the following discussion the term random error magnitude is used. This number represents the variation in a variable where

$$A=A_o(1+R_i(1.0 - 2.0 \text{ RANDOM } (I))) \quad i = 1,2,3,4,5$$

A_o is the value of the variable in the tuned up case
R_i is the random error magnitude
i = 1 error in main cells
i = 2 " " coupling cells
i = 3 " " " constants
i = 4 " " drive phase (given in degrees)
i = 5 " " drive amplitude

The function RANDOM (I) is a computer program which generates a random value in the interval from 0 to 1. The function variable I is used only for the purpose of generating the random numbers and allows reproducing of the distribution by using the same values of I.

For short tanks random variations in frequency need not average over the tank and in general the frequency will not be the same as for a case without errors. In order to obtain meaningful results it is necessary to determine the resonant frequency of the tank before computing the effects of errors. Zero phase in the drive cell is a convenient resonance criteria for use on the computer. This is adequate for errors of 0.1% or less. Computer studies have shown that for these errors zero phase also represents maximum amplitude and correct total phase shift across the tank even with small bandwidth, 2%, and a low accelerating to coupling cell Q ratio, 0.1. For cases with larger errors modes lose definition and are no longer interesting. It is not necessary to search for resonance on the long tank (7469) since the errors should be well averaged for that case and the resonant frequency equal to the drive frequency.

The ability of a tank to tolerate errors was measured by three parameters calculated from the computed values of cell field amplitude and phase; the effective Q of the tank, the amplitude difference, and the phase difference. The effective

Q is self explanatory. The amplitude difference is the maximum difference over the whole tank between main cell amplitudes. The phase difference is the maximum difference between main cell phases modulo π.

Figure 7 shows the configuration of an 800-Mev accelerator using 45 RF drivers and having 7469 cells. Structures of interest are those of 81, 165, and 7469 cells.

The studies on both the 81 and 165 cell tanks have indicated that the three kinds of random errors each have a unique effect on the tank parameters. Although the main cell frequency errors (R1) effect the Q, amplitude difference, and phase difference, the Q is effected only by errors in main cell frequency. An extensive series of computer studies has shown this independence of Q on R2 and R3 even in combination with nonzero R1 terms. Figure 8 demonstrates this for the 165 cell case.

The amplitude difference depends only on R1 and R3. This is the only parameter which is effected by R3. See Fig. 9. These errors introduce random variation in the field amplitudes; however, these random variations are imposed over a much larger consistent error which results in a tilt in the field amplitudes. This result is predictable in the case of the coupling strength errors; they behave like a "random walk".

The phase difference is a function of R1 and R2 and is completely independent of R3. See Fig. 10. The effect of main and coupling cell frequency errors are quite similar. The coupling cell frequency error has a slightly stronger effect. The phase difference is the only parameter significantly effected by coupling cell frequency errors.

TABLE II

Q Ratio	Maximum Error Magnitude (R1, R2, & R3)
0.1	3×10^{-5}
0.2	10^{-4}
0.4	3×10^{-4}
0.6	5×10^{-4}
0.8	10^{-3}
1.0	10^{-3}

Maximum errors in R1, R2, or R3 to maintain amplitude within 3%, Q within 2.5% and phase within 2° for an 81 cell tank with a bandwidth of 2% as a function of the Q ratio.

The 165 cell tank was studied for the case with the Q ratio equal to 0.5 and 4% bandwidth. The results are shown in Figs. 8, 9, and 10. The data was taken from two typical computer runs which differed only in the random numbers generated (each started with a different index for the RANDOM (I) function). The results are qualitatively the same as for an 81 cell case. Assuming

the same tolerances on the tank parameters the maximum random error magnitude is 7×10^{-3}. The interpretation of effects due to errors is relatively simple for single tanks and should be very helpful in initial tuning of segments of a long tank.

The extension of the computer studies to a tank of 7469 cells is essentially trivial; however, the data which is obtained can not be so easily evaluated as in a short tank. In order to determine the usefulness of a long structure its effects on beam dynamics must be studied. Such studies consider the wave form of the tank field and phase errors as well as their amplitude. The error limits quoted here should be evaluated noting that detailed beam dynamics studies have not yet been done. We feel that these values are conservative.

The effects of errors in drive phase and amplitude were studied for the long tank with no other errors. Random error magnitudes of 10% and 10° appear to be easily within tolerable limits. Fig. 11 shows the main cell and drive amplitudes for this case. The case with all R_i's equal to zero is shown in Fig. 12.

The effects of main cell and coupling cell frequency, and coupling constant errors retain the properties discussed above. Errors in all frequencies of magnitude 0.01% and errors in coupling strength of magnitude 0.1% appear to have little effect on the tank. Fig. 13 shows the main cell field and drive amplitude with the errors described above in addition to 10° errors in drive phase and 10% errors in drive amplitude.

Calculating the entire 7469 cell tank as a single chain of resonant circuits is unrealistic. The accelerator would be assembled in eighty-one cell sections, and then into 165 cell sections. Each of these sections will have a well defined resonant frequency which can be tuned. Hence random variations actually occur about 81 cell tanks and not over the whole length of the accelerator.

Any pair of tanks with approximately the same frequency can be coupled together with a drive cell between them. Errors in flatness can be adjusted by adjusting the coupling between the drive cell and each of its two tanks. Each of these 165 cell tanks can be adjusted in frequency by adjusting its temperature. Field amplitude variations can be adjusted by varying both the drive amplitude and the coupling strength of the cell between 165 cell tanks. The initial studies considered none of the above possibilities. The current form of the computer code has provisions for adjusting the average frequencies of each of the 165 cell tanks to the drive frequency.

Future computer studies will consider many of the points discussed above. The next step will be to observe the field distribution for a tank with a given distribution of errors. The drive amplitudes can then be adjusted to achieve

an acceptable field distribution. Then the effects of random variation about the adjusted drive amplitudes can be observed. Normalizing cell frequencies by segments and adjusting coupling constants from tank to tank will also be studied as methods of tuning long tanks with errors.

References

[1] E. A. Knapp, Proceedings of the MURA Conference on Linear Accelerators, Stoughton, Wisconsin, July 20-24, 1964, pp. 31. Available from U.S. Dept. of Commerce, Springfield, Va. TID 4500

[2] D. E. Nagle, ibid pp.21.

[3] D. E. Nagle and E. A. Knapp, Proceedings of the Yale Conference on Proton Linear Accelerators, 1963, pp.171.

[4] D. E. Nagle, P-11 DN/BK/EK-1, Dec. 1964 (Unpublished).
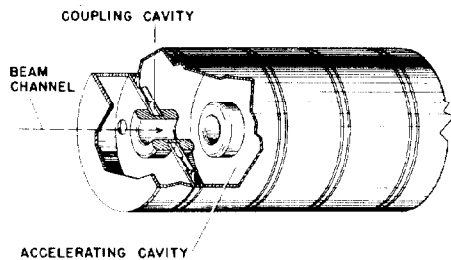
Fig. 1. Magnetically coupled structure with drift tube loaded resonant coupling cells.
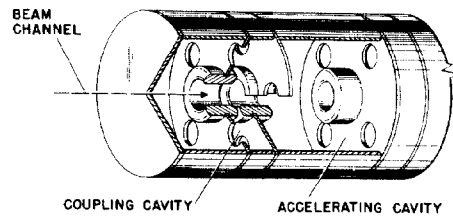
Fig. 2. Magnetically coupled structure with ring-loaded resonant coupling cells.
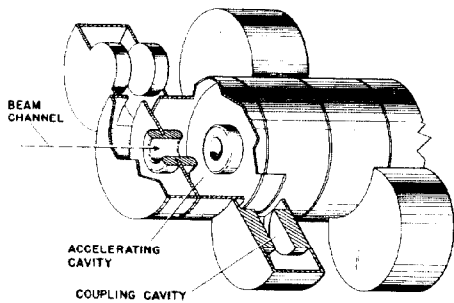
Fig. 3. Side-coupled structure with post-loaded resonant coupling cells.
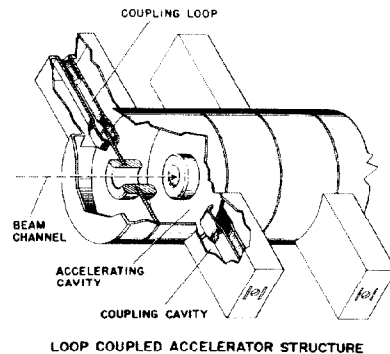
Fig. 4. Strap-coupled structure with resonant parallel plate transmission line coupler.
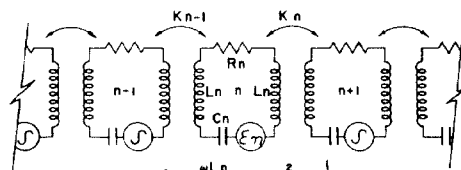
$$Q_n = \frac{\omega L_n}{R_n} \qquad \omega_n^2 = \frac{1}{2 L_n C_n}$$

GENERALIZED EQUIVALENT CIRCUIT

Fig. 5. Chain of magnetically coupled resonant circuits showing notation used in text.

FIELD DISTRIBUTION WITH
COUPLING CONSTANT PERTURBATION
(EXAGGERATED SCALE)
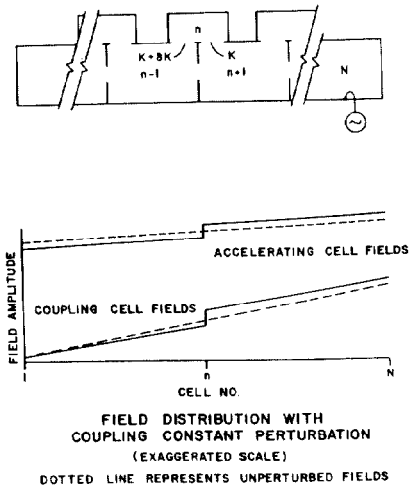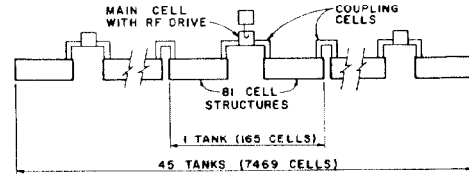DOTTED LINE REPRESENTS UNPERTURBED FIELDS

Fig. 6. Diagram showing result of coupling
constant perturbation on field amplitudes.
Note that there is no relative scale on these
diagrams.

ACCELERATOR CONFIGURATION
USED FOR COMPUTER STUDIES

Fig. 7. Schematic diagram of 800-Mev
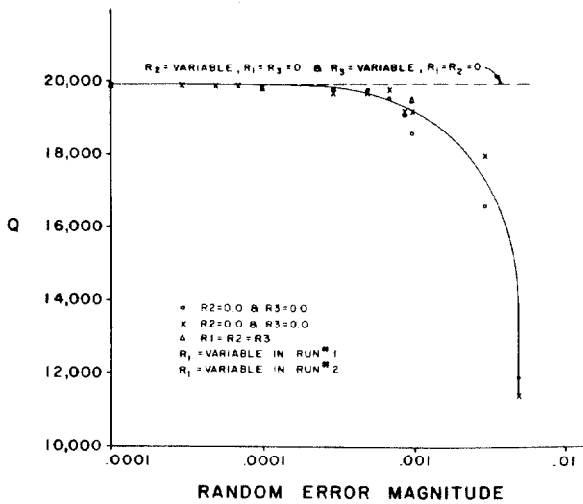accelerator used for computer studies.

RANDOM ERROR MAGNITUDE

Fig. 8. Plot of computed Q as a function of ran-
dom error magnitudes in a 165-cell tank with a Q
ratio of 0.5 and 4% bandwidth. The drive is in
the center accelerating cell. Curves R2 and R3
variable are experimental; however, data points
were too numerous for plotting.

RANDOM ERROR MAGNITUDE
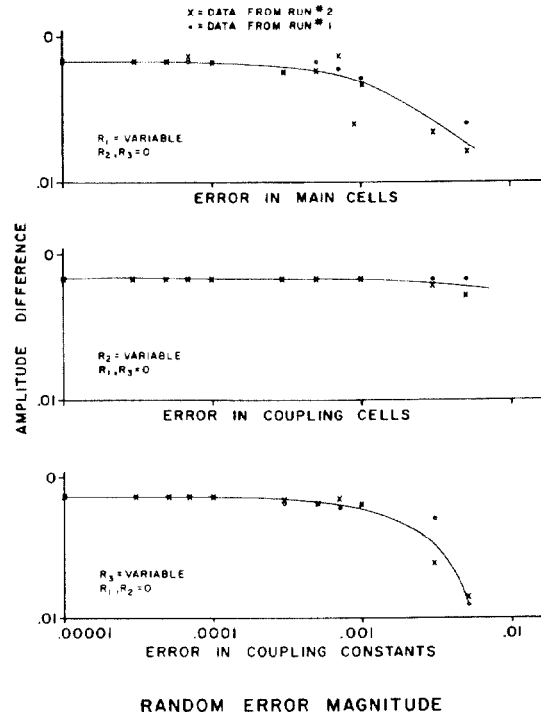
Fig. 9. Plot of computed amplitude difference
as a function of random error magnitude for
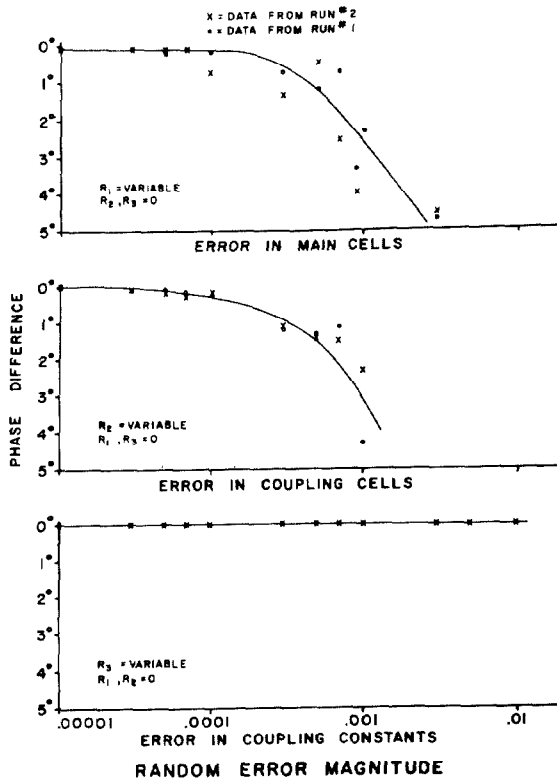the same case as Fig. 8.

Fig. 10. Plot of computed phase differences as a function of random error magnitudes for the same cases as Figs. 8 and 9.
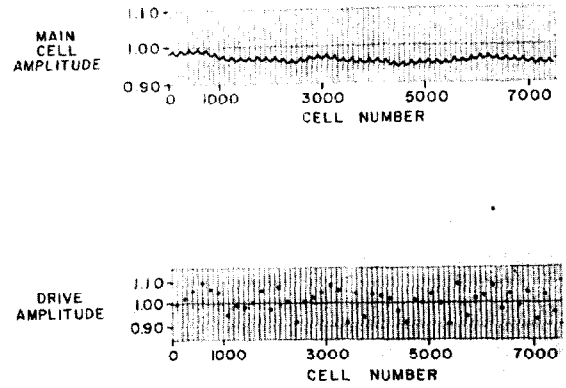

Fig. 11. Plot of accelerating cell and drive amplitude versus cell number for a case with random error magnitudes R1 = 0, R2 = 0, R3 = 0, R4 = 10°, and R5 = 10%. The tank has 7469 cells and 45 RF drivers. The Q ratio is 0.5 and the bandwidth is 4%.
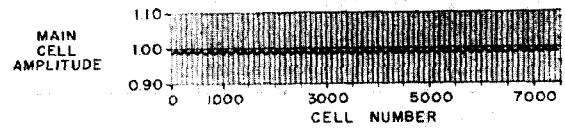

Fig. 12. Plot of accelerating cell amplitude versus cell number for a case with no errors. The tank is the same as for Fig. 11.
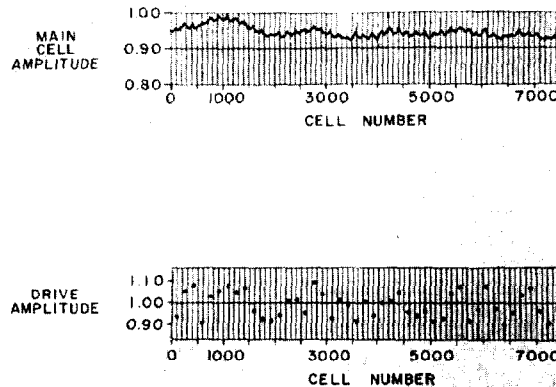

Fig. 13. Plot of accelerating cell and drive amplitude versus cell number for a case with R1 = 0.01%, R2 = 0.01%, R3 = 0.1%, R4 = 10°, and R5 = 10.0%. The tank is the same as for Figs. 11 and 12.